Energy Proceedings
2022
ISSN 2004-2965

Electrochemical characteristics of copper ions in electrochemically-mediated amine regeneration CO_2 capture#

FAN Huifeng[1, 2], MAO Yuanhao[1, 2], WANG Hongxia[1, 2], WU Xaiomei[1*], ZHANG Zaoxiao[1, 2*]

1 School of Chemical Engineering and Technology, Xi'an Jiaotong University, No.28 Xianning West Road, Xi'an 710049, P.R. China

2 State Key Laboratory of Multiphase Flow in Power Engineering, Xi'an Jiaotong University, No.28 Xianning West Road, Xi'an 710049, P.R. China

*Corresponding Author's E-mail: wuxiaomei@xjtu.edu.cn, zhangzx@mail.xjtu.edu.cn, Tel.: +86-29-8266 0689

ABSTRACT

Electrochemically-mediated amine regeneration (EMAR) is a new CO_2 capture technology with the potential to exploit the excellent removal efficiencies of thermal amine scrubbers while reducing parasitic energy losses and capital costs. Copper ions as an important intermediate active substance, it's electrochemical characteristics in EMAR system have a great influence on the efficiency of the system. In this study, a systematic study was carried out on the electrochemical characteristics of copper ions in the EMAR system. Anionic NO_3^- and SO_4^{2+} are identified more suitable for this system than Cl^-. The reduction performance of copper ions will decrease, when the Cu(II) complex is formed with MEA. However, after CO_2 absorption, part of MEA in the solution will react with CO_2 to form carbamate, and the reduction performance of the Cu(II) complex will also be improved. For the cycling performance, a low current density is beneficial to improve the circulation performance of copper ions. The minimum regeneration energy consumption of the EMAR system obtained in the experiment is only 51.26 KJ/mol CO_2, which is extremely competitive compared with thermal scrubbing CO_2 capture process.

Keywords: CO_2 capture, EMAR, copper ions, electrochemical characteristics

1. INTRODUCTION

The anthropogenic release of carbon dioxide (CO_2), has been regard as the most significant contribution to the climate change[1]. To keep within the 2 °C global temperature increasing goal set by the Paris Agreement, it is crucial to cut down CO_2 emission. Carbon capture and storage (CCS) technologies have received considerable attention from the scientific community for the effective minimization of CO_2 emissions to the environment, especially for large point sources[2,3]. Currently, the amine scrubbing process with thermally driven amine regeneration, which has been used in the gas processing industry for decades, is the state-of-the-art technology for carbon capture from large point sources[4]. Despite amine-based thermal scrubbing process is technological maturity, its huge steam consumption during the CO_2 regeneration process, in the range from 2.5 to 4.5 GJ/t CO_2 for practical flue gas treating[4–6], greatly hinders its large-scale industrial application[7], and a new strategy is urgently needed to reduce its energy consumption.

Fundamentally different approaches based on electrochemical processes were recently proposed to drive CO_2 capture and release[8,9]. Electrochemical processes have the potential to be rather energy efficient as they can target molecules directly (instead of the medium surrounding them)[10,11]. Electrochemically-mediated amine regeneration (EMAR) is an emerging new CO_2 capture technology that combine the high removal efficiencies of amine scrubbing and the high efficiency of electrochemical system[12]. The EMAR system has the potential to deduce the energy consumption of the CO_2 amine scrubbing process and minimizing amine degradation by operating the process at low temperature (lower than 100 °C)[10]. Figure 1 depicts the simplified scheme of an EMAR process using monoethanolamine (MEA) as an absorbent and copper as a ligand. The process relies on the competitive binding between CO_2 and a suitable metallic ion (Cu^{2+}) to an amine molecule (MEA). The system is consisting of two sections: the absorption section and desorption section. The absorption section is similar to thermal scrubbing process, and CO_2 is absorbed by amine solvent in an absorption tower. The desorption section of EMAR system is replaced by an electrochemical cell, which consist of an anode chamber and a cathode chamber. The CO_2-rich solvent obtained from absorber is introduced to the anode chamber, where copper ions are generated electrochemically to competitive bind with MEA molecules, at the same time CO_2 is released. The gas

This is a paper for the 14th International Conference on Applied Energy - ICAE2022, Aug. 8-11, 2022, Bochum, Germany.

is subsequently separated through a flash tank located after the anode chamber. Then, the CO_2-lean (Cu-rich) solvent is pumped to the cathode chamber and regenerated via the electrochemical plating of copper from copper-MEA complex (Cu( )). The regenerated MEA can be sent back to the absorber for cycling CO_2 capture. The EMAR system does not rely on steam integration, making it's a plug-and-play unit that can be easily deployed for both scaled-up and scaled-down applications. Researches to date indicate that the EMAR process has the potential to be a viable option for post-combustion CO_2 capture[13].

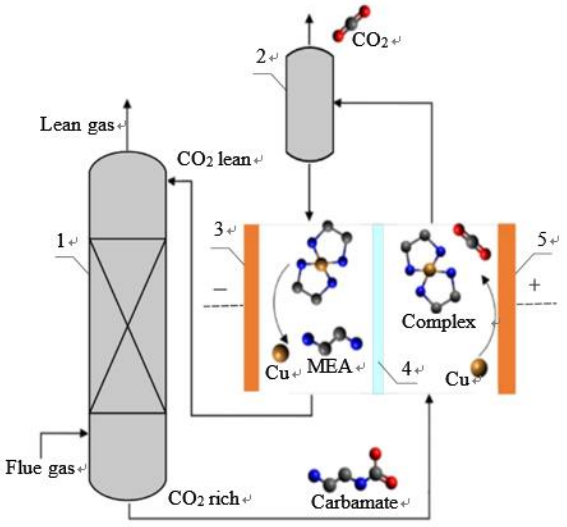

Figure 1 Electrochemically-mediated amine regeneration (EMAR) CO_2 capture process. 1. absorption column, 2. flash tank, 3. Cathode, 4. Membrane, 5. Anode.

A wide variety of efforts to electrochemically mediated CO_2 capture technologies in last two decades have demonstrated the impressing potential of EMAR as a new generation technology for CO_2 capture[12-16]. However, the EMAR technology is still at an early stage for commercial application, some concerns, such as energy-intensive, operating at low current densities, kinetically slow or amine degradation, relating to the long-term operation of the EMAR process must be addressed prior to its practical implementation. Copper ion as an important intermediate active substance in the EMAR process, and its redox reactions shows great effects on energy consumption, energy efficiency and cycling performance of the system.

To study the unclear copper ion redox process and kinetics under different conditions, this work aims to conduct a systematic study on MEA-based electrochemical CO_2 capture process and discuss the copper cycling performance in EMAR process. According to the previous research results, the anode and cathode reactions of the reaction system are carried out step by step, the cathode reaction is the control step of the whole process, and the anode and cathode electrode reactions are controlled by diffusion and charge transfer[17]. Hence, the reduction characteristics and kinetic characteristics of copper ions were studied in this work, and the effects of anions, amine and CO_2 were discussed. Furthermore, the circulation performance of copper ions was comprehensively discussed in this work to show its applicability in the EMAR CO_2 capture process.

2. MATERIALS AND METHODS

2.1 Experimental

2.1.1 Materials and electrolyte preparation

All chemicals including MEA (Sigma Aldrich, AR), $Cu(NO_3)_2{\cdot}xH_2O$ (Sigma Aldrich, AR), $CuSO_4{\cdot}5H_2O$ (Sigma Aldrich, AR), $CuCl_2{\cdot}2H_2O$ (Sigma Aldrich, AR), KNO_3 (Sigma Aldrich, AR) were purchased from Sigma-Aldrich without further purification. Deionised water (Millipore, 18 MΩ cm) was used to prepare solutions.

When preparing the solution, deionized water is used as the benchmark. To ensure a good conductivity of solution, KNO_3 was used as the supporting electrolyte. Copper salt ($Cu(NO_3)_2{\cdot}xH_2O$, $CuSO_4{\cdot}5H_2O$ and $CuCl_2{\cdot}2H_2O$) were added to provide divalent copper ions and different anions. MEA was used as CO_2 absorbent and to complex with copper ions. To make it clear, the detailed information about how the electrolyte solution for different tests were prepared are shown in the results and discussion section. To get CO_2-rich solution, pure CO_2 (99.99 vol%) was bubbled into the prepared electrolyte solution in a gas washing bottle at a flow rate of 500 sccm, which was controlled by Airoboost mass flow controllers. The absorption temperature for electrochemical tests and copper cycle tests were kept at 25 and 40 respectively, which was controlled by a water bath. After absorption, the electrolyte solution was purged with N_2 to remove the dissolved O_2 or other physically dissolved gases. The data of CO_2 loading (L_{CO2}) in solvents, defined as the moles of CO_2 absorbed per one mole of MEA, were determined by measuring the volume of CO_2 gas that was pushed out by excessive acid (H_2SO_4, 25%). This CO_2-loading measurement method has been validated by the standard method of Association of Official Analytical Chemists (AOAC), with an average error of ±3% between the actual and measured results, indicating its validity. To reduce errors caused by the vaporization of the solution, the gas outlet was connected to a jacketed coil condenser. Necessary sealing measures were taken to avoid the solution in contact with air.

2.1.2 Electrochemical measurements

Electrochemical measurements were carried out in a 100 mL cell. Experiments were conducted by an electrochemical workstation (Corrtest Instruments, CS2350). Three electrodes system was used in all electrochemical tests. Copper (GB T2, ≥99.9%) and glassy carbon were used as electrodes in electrochemical tests. A saturated silver/silver chloride (Ag/AgCl) reference electrode was introduced in the solution by a Luggin capillary. Before every experiment the electrodes were grounded with 2000 grit silicon carbide paper and then polished with a diamond polishing agent (1.0 μm, 0.3 μm, 0.05 μm) in turn. After polishing, the electrodes were cleaned with deionized water and isopropyl alcohol in an ultrasonic bath.

The electrochemical reaction under various electrolyte conditions was analyzed by using cyclic voltammetry (CV). Chronocoulometer (CC) tests were used to study the diffusion coefficients and the reaction rate constants of ions. After reaching the test environments, the tests started with open circuit potential (OCP) measurements. The OCP was recorded until it reached a steady state (0.5 mV between successful voltage readings). Cyclic voltammetry (CV) experiments were conducted at the scan rate of 70 mV/s. Chronocoulometer (CC) tests were carried out at different overpotentials. Nitrogen was injected into the solution for 10 mines before the tests to discharge the dissolved oxygen in the solution, and all the tests were carried out in a nitrogen atmosphere. To ensure the accuracy of the measurements, all the experiments were repeated three times and the average values were used in this work.

2.1.3 Copper cycling performance measurements

In order to reduce the interference between anode and cathode reactions in measurement process. Copper cycling performance measurements were carried out in an H-cell with a single cell volume of 50 mL, which was divided into cathode and anode chamber by sand core. The electrolytic cell was a three-electrode system assembly with a saturated silver/silver chloride (Ag/AgCl) reference electrode, working electrode and counter electrode made of copper with a surface area of 1 cm^2.

The experiments were carried out at a constant current, and the result of cell voltage and current *vs*. time were recorded. Before and after the experiments, the cathode and anode were dried and weighed separately on an electronic balance GL224I-1SCN with accuracy up to 0.1 mg, and the data of CO_2 loading (L_{CO2}) in solvents were measured. The changes of electrode surface were observed by scanning electron microscope (SEM).

2.2 Kinetic parameter determination

2.2.1 The diffusion coefficients *of copper ions*

Chronocoulometer (CC) tests were used to study the diffusion coefficients of copper ions in solution. The potential of working electrode was set as E_1 at the initial stage which represents there is no reaction occurred in solvent. Then the potential changed to E_2, which is the reduction peak of solvents and keep at E_2 for 5 s. The relationship between electric quantity and time agrees well with the Anson equation as following [18,19].

$$Q = \frac{2nFAD_{\mathrm{O}}^{1/2}c_{\mathrm{O}}^{*}}{\pi^{1/2}}t^{1/2} + Q_{\mathrm{dl}} \quad (1)$$

where *n* is the number of electrons transferred in copper ions reduction process; *F* is the Faraday's constant; *A* is the active area of the working electrode which was tested by 2 mmol/L $K_3Fe(CN)_6$ solvent; D_O is the diffusion coefficient of reaction particles; c_O* is the concentration of reaction particles; Q_{dl} is the charge capacity of double electrode layer. The diffusion coefficient of reaction particles in solution can be calculated according to the slop of asymptote of curve *Q* and $t^{1/2}$.

2.2.2 The reaction rate constants

The reaction rate constants were measured by conducing chronocoulometer (CC) tests with different step potentials (E_2) in the rising region of the cyclic voltammetry. During the tests, the electrode reaction cannot reach the limit diffusion control degree, and the dynamic process of charge transfer at the electrode interface can be obtained completely or partially in a short response time. At this point, the electric quantity response of quasi-reversible reaction satisfies the equation as following[19].

$$Q = \frac{2nFAD_{\mathrm{O}}^{1/2}c_{\mathrm{O}}^{*}}{\pi^{1/2}} \times \left[\exp(H^2 t)\mathrm{erfc}(Ht^{1/2}) + \frac{2Ht^{1/2}}{\pi^{1/2}} - 1 \right] \quad (2)$$

where $H = (k_{\mathrm{f}} / D_{\mathrm{O}}^{1/2}) + (k_{\mathrm{b}} / D_{\mathrm{R}}^{1/2})$, D_{O} and D_{R} are the diffusion coefficient of redox electric pair respectively; k_{f} and k_{b} are the reaction rate constants of reduction and oxidation process respectively. When the $Ht^{1/2} > 5$, the following equation can be obtained.

$$Q = nFAk_{\mathrm{f}}c_{\mathrm{O}}^{*}\left(\frac{2t^{1/2}}{H\pi^{1/2}} - \frac{1}{H^2}\right) \quad (3)$$

Then the reaction rate constants of electrode can be calculated according to the slop and intercept of asymptote of curve Q and $t^{1/2}$.

2.3 Copper cycling performance evaluation parameters

2.3.1 Desorption energy consumption

Desorption energy consumption was calculated as the ratio between the amount of CO_2 desorption and its

actual energy consumption. The Desorption energy consumption (W, kJe/mol CO_2) in the EMAR process was calculated by:

$$W(\mathrm{kJ_e/mol\ CO_2}) = \frac{\int_0^{t_0} UIdt}{\Delta n_{CO_2}} \quad (4)$$

where U is the cell voltage; I is the applied current; t_0 is the reaction time; Δn_{CO2} is the moles of CO_2 desorption.

2.3.2 Faradaic efficiency

Faraday efficiency was expressed as the ratio of the actual charge involving Cu redox reaction to its theoretical charge. The experimental Faraday efficiency could be divided into anode Faraday efficiency (AFE) and cathode Faraday efficiency (CFE), which are determined as follows:

$$\mathrm{AFE} = \frac{2\Delta n_A F}{\int_0^{t_0} Idt} \quad (5)$$

$$\mathrm{CFE} = \frac{2\Delta n_C F}{\int_0^{t_0} Idt} \quad (6)$$

where Δn_A and Δn_C are the moles of Cu lost in the anode in the experiment or gained in the cathode, respectively.

3. RESULTS AND DISCUSSIONS

3.1 Electrochemical characteristics of copper ions in EMAR

3.1.1 Effects of different anions on copper redox reaction

In order to study the influence of anions on copper redox reaction, three kind of copper salts $Cu(NO_3)_2{\cdot}xH_2O$, $CuSO_4{\cdot}5H_2O$ and $CuCl_2{\cdot}2H_2O$ were selected for performance comparison. The solutions were prepared with 0.7 mol/kg (H_2O) of KNO_3. The concentrations of each copper salt ($Cu(NO_3)_2{\cdot}xH_2O$, $CuSO_4{\cdot}5H_2O$ and $CuCl_2{\cdot}2H_2O$) were taken as 0.07 mol/kg(H_2O), 0.14 mol/kg(H_2O) and 0.21 mol/kg(H_2O), respectively. Figure 2 shows cyclic voltammetry curves for different copper salts. Cyclic voltammetry was used to test the redox reaction characteristics of copper in different solutions.

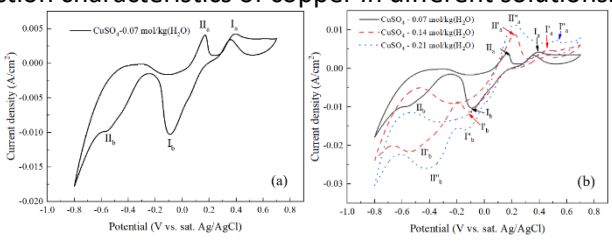

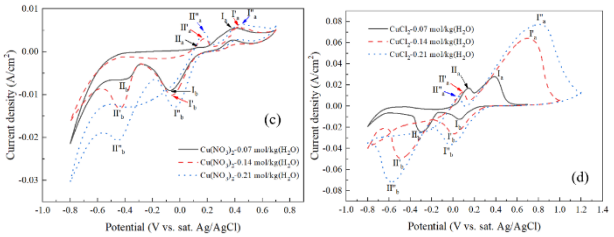

Figure 2 Cyclic voltammetry curves for different copper salts. (a) Cyclic voltammetric curve for $CuSO_4$ with a concentration of 0.07 mol/kg (H_2O). (b), (c) and (d) Cyclic voltammetric curves of $CuSO_4$, $Cu(NO_3)_2$ and $CuCl_2$ solutions at different copper ion concentrations, respectively.

Figure 2(a) shows the cyclic voltammetry curve for $CuSO_4$ with a concentration of 0.07 mol/kg (H_2O), in which the oxidation peak Ia (0.395 V) and the reduction peak Ib (-0.091 V) are a pair of redox peaks with an average peak potential of 0.152 V. According to the standard electrode potential meter, the reaction peaks I_a and I_b correspond to the oxidation of Cu to Cu^{2+} and the reduction of Cu^{2+} to Cu, respectively. The oxidation peak II_a (0.169 V) and the reduction peak II_b (-0.564 V) are a pair of redox peaks with an average peak potential of -0.1975 V. The reaction peaks II_a and II_b correspond to the oxidation of Cu^+ to Cu^{2+} and the reduction of Cu^{2+} to Cu^+, respectively.

Figure 2(b), (c) and (d) show the cyclic voltammetry curves of $CuSO_4$, $Cu(NO_3)_2$ and $CuCl_2$ solutions at different copper ions concentrations, respectively. The peak current and potential of redox of Cu/Cu^{2+} increased at higher copper ions concentrations, which indicated that diffusion is the electrode control step in this reaction. At the same time, it can be observed that the mean and amplitude of the peak potential and current density of the $CuCl_2$ solution are significantly larger than those of the $CuSO_4$ and $Cu(NO_3)_2$ solutions, indicating that the redox reaction of Cu/Cu^{2+} is more difficult to occur in $CuCl_2$ solution. The existence of the redox reaction of Cu^+/Cu^{2+} will reduce the charge required for the redox reaction of Cu/Cu^{2+}, which in turn reduces its reaction rate. Compared to $CuSO_4$ and $Cu(NO_3)_2$ solutions, the peak potential of the oxidation process from Cu^+ to Cu^{2+} in $CuCl_2$ solution decreases with the increasing of the $CuCl_2$ concentration in the solution. The initial peak potential of the reduction process from Cu^{2+} to Cu^+ in $CuCl_2$ solution is smaller, indicating that it occurs more easily. Therefore, $CuSO_4$ and $Cu(NO_3)_2$ are more suitable as copper salts for the EMAR system.

3.1.2 Effects of MEA on copper reduction performance

During the working process of the EMAR system, the copper ions in the solution will coordinate with the MEA to form a copper-amine complex (Cu(II)), which further

promotes the desorption of CO_2, and then the copper-amine complex (Cu(II)) get electrons at the cathode, the copper ions are reduced to copper. In the previous section, we studied the redox characteristics of copper ions in aqueous solution and the influence of the presence of different anions on their redox characteristics. On this basis, it is necessary to study the effect of MEA on the reduction characteristics of Cu(II).

The solutions were prepared with 0.7 mol/kg (H_2O) of KNO_3. The concentration of copper salt ($CuSO_4{\cdot}5H_2O$) was taken as 0.07 mol/kg(H_2O), and MEA concentrations were 0.3 mol/kg(H_2O) and 0.6 mol/kg(H_2O). Cyclic voltammetry experiments were conducted between -0.8 V and 0.7 V vs. sat. Ag/AgCl to test the redox reaction characteristics of copper in different solutions. Chronocoulometer tests were conducted at the reduction peak potential to study the diffusion coefficients and the reaction rate constants of Cu^{2+}/ Cu(II) in different solutions.

Figure 3 shows the reduction peaks of Cu^{2+}/ Cu(II) in different solutions. It can be seen that peak 1 (-0.08 V) represents the reduction reaction of copper ions (Cu^{2+}) to copper (Cu), and peak 2 (-0.50 V) and 3 (-0.49 V) represent the reduction of copper amine complex (Cu(II)) to form copper (Cu) under a MEA concentration of 0.3 mol/kg(H_2O) and 0.6 mol/kg(H_2O), respectively. After Cu^{2+} combines with MEA to form a complex, the reduction peak potential moves to the negative direction, from -0.08 V to -0.50 V, indicating that the reduction reaction is more difficult to occur. When the concentration of MEA increased from 0.3 mol/kg (H_2O) to 0.6 mol/kg (H_2O), the reduction peak potentials were almost kept the same, which indicate that the excess MEA has little effect on the peak potential of the reduction reaction of the copper amine complex (Cu(II)).

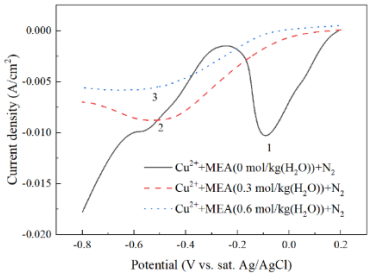

Figure 3 the reduction peaks of Cu^{2+}/ Cu(II) in different solutions

Table 1 shows Cu^{2+}/ Cu(II) diffusion coefficients in different solutions. The results show that before and after Cu^{2+} complex with MEA, the diffusion coefficient of copper ions decreased from 2.277×10^{-5} cm^2/s to 2.095×10^{-5} cm^2/s, which indicate that the ionic diffusion property becomes worse after the formation of complex. With the increase of MEA concentration, the diffusion coefficient of copper ions further decreases, indicating that high MEA concentration is not conducive to the diffusion of the complex.

Table 1 Cu^{2+}/ Cu(II) diffusion coefficients in different solutions.

Reduction peak	Diffusion coefficient of copper ions $\times10^{-5}$ $cm^2{\cdot}s^{-1}$
$Cu^{2+}+N_2$	2.277
Cu^{2+}+MEA (0.3 mol/kg(H_2O))+N_2	2.095
Cu^{2+}+MEA (0.6 mol/kg(H_2O))+N_2	1.978

Table 2 shows the reaction rate constants of Cu^{2+}/Cu(II) at different step potential difference. The reaction rate constants of step potential difference before complex (7.495×10^{-6} m/s→4.233×10^{-6} m/s) are greater than those after complex (5.515×10^{-6} m/s→4.116×10^{-6} m/s), the specific kinetic data also show that the complex rate changes slowly under the same step potential change, which indicates that the reduction reaction after complex is more controllable, which is beneficial to the cathode-controlled generation of copper. With the increase of MEA concentration, the situation is further improved.

Table 2 the reaction rate constants of Cu^{2+}/ Cu(II) at different step potential difference.

Reduction peak	Step potential difference /V	Reaction rate constant$\times10^{-6}$ $m{\cdot}s^{-1}$
$Cu^{2+}+N_2$	0.04	7.495
	0.08	5.035
	0.12	4.233
Cu^{2+}+MEA (0.3 mol/kg(H_2O))+N_2	0.04	5.515
	0.08	4.614
	0.12	4.116
Cu^{2+}+MEA (0.6 mol/kg(H_2O))+N_2	0.04	4.342
	0.08	3.958
	0.12	3.653

3.1.3 Effects of CO_2 on copper reduction performance

In the EMAR process, the desorption solution is CO_2 rich solution. In the previous sections, we studied the redox characteristics of Cu^{2+} in aqueous solution and the

effect of MEA on copper ions reduction performance. On this basis, it is necessary to study the effect of CO_2 on the reduction characteristics of copper.

The solutions were prepared with 0.7 mol/kg (H_2O) of KNO_3. The concentrations of copper salt ($CuSO_4 \cdot 5H_2O$) was taken as 0.07 mol/kg(H_2O), and MEA was 1.0 mol/kg(H_2O). By controlling the CO_2 inflow time, CO_2-rich solution with different loadings can be obtained. We tested three kinds of solutions: CO_2-saturated, unsaturated and free states. Cyclic voltammetry experiments were conducted between -0.9 V and 1.0 V vs. sat. Ag/AgCl.

Figure 4 shows the reduction peaks of Cu^{2+}/ Cu(II) of different CO_2 loadings solutions. In MEA aqueous solution without CO_2, the reduction peak of the copper-amine complex (Cu(II)) is peak 1 (-0.52 V). When the solution absorbs CO_2, the cathodic reduction peak shifts to higher potential， as a result of rapid reaction of MEA with CO_2 to form a carbamate. The peak current density is also observed to increase significantly with the increase of CO_2 loadings, which due to the formation of carbamate will enhance the conductivity of the solution.

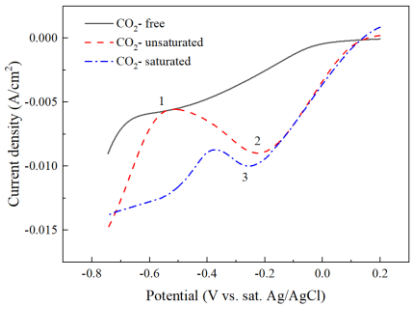

Figure 4 Reduction peaks of Cu^{2+}/ Cu(II) in different CO_2 loads solutions.

In the solution of CO_2 free, the reduction peak potential is -0.52 V. When the solution absorbed CO_2, the reduction potential increases to -0.22 V at the unsaturated state and -0.25 V at the saturated state, which indicate. This phenomenon indicates that the reduction reaction is more likely to occur. Meanwhile, as shown in Table 3 and Table 4, when the solution absorbed CO_2, the diffusion coefficient increases from 2.095×10^{-5} cm^2 /s at CO_2 free state to 1.865×10^{-5} cm^2/s at the unsaturated state and 1.733×10^{-5} cm^2/s at the saturated state. The reaction rate constants at different step potentials (5.515×10^{-6} m/s→4.116×10^{-6} m/s) at CO_2 free state were smaller than that (9.732×10^{-6} m/s→4.974×10^{-6} m/s) at the unsaturated state and (11.610×10^{-6} m/s→5.730×10^{-6} m/s) at the saturated state.

In conclusion, when the solution absorbed CO_2, the electrode diffusion controllability is stronger and the reaction controllability becomes worse. Therefore, we can promote the copper ion reduction reaction by appropriately increasing the CO_2 loading (L_{CO2}) in the solution

Table 3 Cu^{2+}/ Cu(II) diffusion coefficients in different CO_2 loads solutions.

Reduction peak	Diffusion coefficient of copper ions $\times10^{-5}$ $cm^2 \cdot s^{-1}$
CO_2-free	2.095
CO_2- unsaturated	1.865
CO_2- saturated	1.733

Table 4 the reaction rate constants of Cu^{2+}/Cu(II) at different step potential difference.

Reduction peak	Step potential /V	Reaction rate constant$\times10^{-6}$ $m \cdot s^{-1}$
CO_2-free	0.04	5.515
	0.08	4.614
	0.12	4.116
CO_2- unsaturated	0.04	9.732
	0.08	8.043
	0.12	4.974
CO_2- saturated	0.04	11.610
	0.08	7.600
	0.12	5.730

3.2 Cycling performance and energy consumption

3.2.1 *Analysis of copper cycling performance*

The cyclic performance of the EMAR system under different working conditions are studied. The concentration of KNO_3 was 0.7 mol/kg (H_2O) and the concentration of $CuSO_4$ was 0.07 mol/kg (H_2O), the MEA concentration was 7 mol/kg(H_2O), and then saturated CO_2 was absorbed at a temperature of 40 °C to obtain the desired solution. The desorption is carried out according to the galvanostatic method. In order to ensure the same amount of electron transferred, the desorption is carried out under three working conditions: 0.01 A/cm^2 - 9000 s, 0.02 A/cm^2 - 4500 s and 0.03 A/cm^2 -3000 s.

Table 5 The electrode Faraday efficiency and desorption energy consumption

	AFE / %	CFE / %	*W* / kJe/mol CO_2

0.01 A/cm^2 - 9000 s	6.87	13.40	51.26
0.02 A/cm^2 - 4500 s	20.26	50.24	89.06
0.03 A/cm^2 -3000 s	27.80	76.69	103.45

The electrode Faraday efficiency and desorption energy consumption are shown in the table 5. It can be found that under the three working conditions tested, the AFE and CFE both tend to increase with the applied current density increased from 0.01 A/cm^2 to 0.03 A/cm^2., the AFE increases from 6.87% to 27.80% and the CFE increases from 13.40% to 76.69%. Meanwhile it also can be found that the AFE is always less than the CFE, indicating that electrode Faraday efficiency is strongly limited by the kinetically sluggish anodic copper dissolution reaction. This phenomenon becomes more obvious with the increase of current density. As the reaction progress, the copper loading ($L_{Cu(II)}$) in solution will decrease continuously, which leads to a lower $L_{Cu(II)}$ in the absorption process. According to the absorption process study, a lower $L_{Cu(II)}$ in the absorption process would reduce potential precipitation of $CuCO_3$ and a higher absorption kinetics. These issues are conductive to improve CO_2 capture efficiency and decrease capital input of the absorber.

As for desorption energy consumption, operating at very low current density is ineffective due to the higher salt ion leakage and leading to lower CO_2 desorption efficiency. On the other hand, at high current density, the ohmic voltage losses increase, leading to an undesirable higher energy consumption. we can see that the desorption energy consumption sharply increases from 51.26 kJe/mol(CO_2) to 101.739 kJe/mol(CO_2) with the applied current density increased from 0.01 A/cm^2 to 0.03 A/cm^2.

Figure 5 shows the SEM graphs of anode and cathode electrode surface after desorption under three working conditions. For the anode, a porous structure is formed on the electrodes surface during the electrochemical copper dissolution process. With the increase of current density, the porous structure became more intensive. As for cathode, a lot of newly deposited columnar crystals cover the electrode surface which have been verified by EDS results are copper. With the increase of current density, the newly deposited copper crystals on electrode surface becomes denser. The above shows that better cyclic performance of copper can be realized by appropriately increasing the current in the range of experimental conditions.

Therefore, considering the economy of the system and the circulation performance of copper, a current density of 0.02 A/cm^2 is suggested in this work.

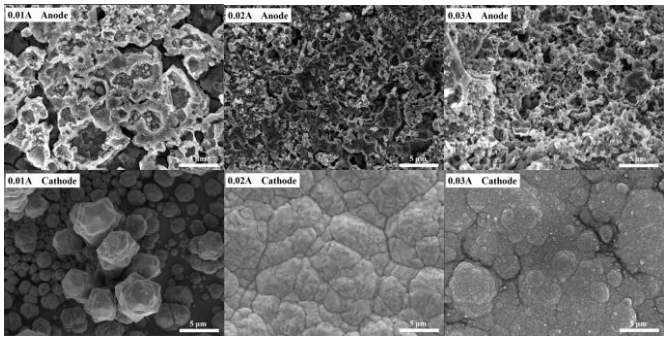

Figure 5 the SEM graphs of anode and cathode electrode surface after desorption under different conditions

4. CONCLUSIONS

Electrochemically-mediated amine regeneration (EMAR) is an emerging new CO_2 capture technology that combine the high removal efficiencies of amine scrubbing and the high efficiency of electrochemical system. However, the EMAR technology is still at an early stage for commercial application. Copper ions as an important intermediate active substance, it's electrochemical characteristics in EMAR system have a great influence on the efficiency of the system. Through the systematic study on the electrochemical characteristics of copper ions in EMAR system, some practical and intentional conclusions have been obtained.

As for the effect of anions, the influence of anionic NO_3^- and SO_4^{2+} on copper redox reaction performance are identified better for EMAR system than Cl^-. With the adding of MEA in solution, due to the interaction of copper ions and MEA, a copper-amine complex (Cu(II)) is formed, and the reduction performance of copper ions is worse than before the formation of the complex. However, with the introduction of CO_2, part of MEA in the solution will react with CO_2 to form carbamate, and the reduction performance of the Cu(II) complex will be improved. For the cycling performance, a low current density is beneficial to improve the circulation performance of copper ions. The regeneration energy consumption of the EMAR system at a current density of 0.01 A/cm^2 is only 51.26 KJ/mol CO_2, which is extremely competitive compared with thermal scrubbing CO_2 capture process. However, considering the economy of the system and the circulation performance of copper, a current density of 0.02 A/cm^2 is suggested in this work.

ACKNOWLEDGEMENT

Financial supports of the National Natural Science Foundation of China (Nos. 42141011, 52106209, 51876150 and 52050027) are gratefully acknowledged. This work is also supported by the China Postdoctoral Science Foundation (2020M673390) and Fundamental

Research Funds for the Central Universities (xjh012020034).

REFERENCE

[1] Engelbrecht F, Monteiro P. The IPCC Assessment Report Six Working Group 1 report and southern Africa: Reasons to take action[J]. SOUTH AFRICAN JOURNAL OF SCIENCE, 2021, 117(11–12).

[2] Liu Z, Deng Z, Davis S J, et al. Monitoring global carbon emissions in 2021[J]. Nature Reviews Earth & Environment, London: Springernature, 2022, 3(4): 217–219.

[3] Friedlingstein P, Jones M W, O'Sullivan M, et al. Global Carbon Budget 2021[J]. Earth System Science Data, Gottingen: Copernicus Gesellschaft Mbh, 2022, 14(4): 1917–2005.

[4] Notz R, Mangalapally H P, Hasse H. Post combustion CO2 capture by reactive absorption: Pilot plant description and results of systematic studies with MEA[J]. International Journal of Greenhouse Gas Control, Oxford: Elsevier Sci Ltd, 2012, 6: 84–112.

[5] Harbou I, Mangalapally H P, Hasse H. Pilot plant experiments for two new amine solvents for post-combustion carbon dioxide capture[J]. International Journal of Greenhouse Gas Control, Oxford: Elsevier Sci Ltd, 2013, 18: 305–314.

[6] Rabensteiner M, Kinger G, Koller M, et al. Pilot plant study of aqueous solution of piperazine activated 2-amino-2-methyl-l-propanol for post combustion carbon dioxide capture[J]. International Journal of Greenhouse Gas Control, Oxford: Elsevier Sci Ltd, 2016, 51: 106–117.

[7] Wu X M, Qin Z, Yu Y S, et al. Experimental and numerical study on CO2 absorption mass transfer enhancement for a diameter-varying spray tower[J]. Applied Energy, Oxford: Elsevier Sci Ltd, 2018, 225: 367–379.

[8] Khurram A, He M, Gallant B M. Tailoring the Discharge Reaction in Li-CO2 Batteries through Incorporation of CO2 Capture Chemistry[J]. Joule, 2018, 2(12): 2649–2666.

[9] Rahimi M, Catalini G, Puccini M, et al. Bench-scale demonstration of CO_2 capture with an electrochemically driven proton concentration process[J]. RSC Advances, 2020, 10(29): 16832–16843.

[10] Stern M C, Simeon F, Herzog H, et al. Post-combustion carbon dioxide capture using electrochemically mediated amine regeneration[J]. Energy & Environmental Science, Cambridge: Royal Soc Chemistry, 2013, 6(8): 2505–2517.

[11] Wang M, Herzog H J, Hatton T A. CO2 Capture Using Electrochemically Mediated Amine Regeneration[J]. Industrial & Engineering Chemistry Research, Washington: Amer Chemical Soc, 2020, 59(15): 7087–7096.

[12] Stern M C, Hatton T A. Bench-scale demonstration of CO2 capture with electrochemically-mediated amine regeneration[J]. RSC Advances, The Royal Society of Chemistry, 2014, 4(12): 5906–5914.

[13] Rahimi M, Diederichsen K M, Ozbek N, et al. An Electrochemically Mediated Amine Regeneration Process with a Mixed Absorbent for Postcombustion CO2 Capture[J]. Environmental Science & Technology, American Chemical Society, 2020, 54(14): 8999–9007.

[14] Eltayeb A O, Stern M C, Herzog H, et al. Energetics of Electrochemically-mediated Amine Regeneration[J]. Energy Procedia, 2014, 63: 595–604.

[15] Liu G X, Yu Y S, Hong Y T, et al. Identifying electrochemical effects in a thermal–electrochemical co-driven system for CO_2 capture[J]. Physical Chemistry Chemical Physics, 2017, 19(20): 13230–13244.

[16] Cheng C, Li K, Yu H, et al. Amine-based post-combustion CO2 capture mediated by metal ions: Advancement of CO2 desorption using copper ions[J]. Applied Energy, 2018, 211: 1030–1038.

[17] Wu X, Fan H, Sharif M, et al. Electrochemically-mediated amine regeneration of CO2 capture: From electrochemical mechanism to bench-scale visualization study[J]. Applied Energy, 2021, 302: 117554.

[18] Perez-Gonzalez V H. Induced Electrokinetics: Fundamentals and Applications 2021[J]. Electrophoresis, Hoboken: Wiley, 2021, 42(23): 2421–2422.

[19] Bard AJ, Faulknler L R. Electrochemical methodsfundamentals and applications [M]. Shao Yuanhua, Zhu Guoyi, Dong Xiandui, transl. Beijing: Chemical Industry Press, 2005,67:145 171. (in Chinese).